Protist, Vol. 158, 277—293, July 2007
http://www.elsevier.de/protis
Published online date 13 June 2007

Protist

ORIGINAL PAPER

Synchroma grande spec. nov. (Synchromophyceae class. nov., Heterokontophyta): An Amoeboid Marine Alga with Unique Plastid Complexes

Susanne Horn[a], Katrin Ehlers[b], Guido Fritzsch[c], María Candelaria Gil-Rodríguez[d], Christian Wilhelm[a,1], and Reinhard Schnetter[b,1]

[a]Institut für Biologie I, Abteilung Pflanzenphysiologie, Universität Leipzig, Johannisallee 21-23, 04103 Leipzig, Germany
[b]Institut für Allgemeine Botanik und Pflanzenphysiologie, Justus-Liebig-Universität, Senckenbergstr. 17, 35390 Giessen, Germany
[c]Interdisciplinary Center for Bioinformatics, University of Leipzig, Härtelstr. 16-18, 04107 Leipzig, Germany
[d]Departamento de Biología Vegetal, Universidad de La Laguna, E-38071 La Laguna, Spain

Submitted October 16, 2006; Accepted February 24, 2007
Monitoring Editor: Robert A. Andersen

Chromist algae including the Heterokontophyta are supposed to have evolved monophyletically by secondary endosymbiosis from a eukaryotic host cell that engulfed a eukaryotic red alga. The red algal endosymbiont was then reduced to a secondary plastid surrounded by four enveloping membranes. On the basis of the amoeboid marine alga *Synchroma grande* gen. et spec. nov., the Synchromophyceae are described here as a new class of Heterokontophyta. Their taxonomic position is characterized by 18S rRNA and *rbc*L gene phylogenies, morphology, and pigment composition. The so far unique feature of the Synchromophyceae is the occurrence of conspicuous chloroplast complexes representing multiplastidic red secondary endosymbionts. In these remarkable secondary endosymbionts, several primary chloroplasts are aggregated in a common periplastidial compartment and are collectively enveloped by an additional outer membrane pair. The discovery of this novel plastid morphology is highly relevant for research on algal evolution and is discussed in terms of the postulated monophyletic origin of Chromista.

Key words: amoeboid alga; Chromista; Heterokontophyta; secondary endosymbiont; *Synchroma*; Synchromophyceae.

Introduction

The Heterokontophyta sensu van den Hoek (1978) constitute a remarkable group of algae including ecologically important groups, e.g. the Bacillariophyceae (diatoms), the Chrysophyceae (golden algae), and the Phaeophyceae (brown algae). There is considerable variation in the circumscription of higher-ranking taxa comprising this algal group, e.g. Heterokonta (Cavalier-Smith 1986), Stramenopiles (Patterson 1989), Chromista (Cavalier-Smith 1981), and Straminipila (Dick 2001). Thus, we avoid to use these terms and refer to the Heterokontophyta sensu van den Hoek, only.

[1]Corresponding authors;
e-mails cwilhelm@rz.uni-leipzig.de (C. Wilhelm),
Reinhard.Schnetter@bot1.bio.uni-giessen.de (R. Schnetter).

doi:10.1016/j.protis.2007.02.004

The Heterokontophyta contain characteristic xanthophylls as the taxonomically relevant pigments besides chlorophylls *a* and *c* in their secondary plastids (Andersen 2004). In the Eustigmatophyceae, however, chlorophyll *c* is missing (Andersen 2004). The Heterokontophyta include a large variety of unicellular and multicellular algal organisms with a high morphological diversity. In recent years, more detailed studies on this diversity resulted in taxonomic rearrangements within the group as well as in descriptions of numerous new genera and species (Andersen et al. 2002; Bongiorni et al. 2005; Eikrem et al. 2004; Kawachi et al. 2002a; O'Kelly 2002), and even of several new classes of Heterokontophyta (Kawachi et al. 2002b; Kawai et al. 2003; Moriya et al. 2002). Molecular analyses of environmental samples already indicated that the discovery of further novel taxa can be expected (Massana et al. 2002). Here, we present a new class of Heterokontophyta, the Synchromophyceae, whose conspicuous plastid morphology can deliver new insights into evolution, cytology, and physiology of the Heterokontophyta in particular and of secondary plastid-bearing algae in general.

In algae, the occurrence of secondary plastids characterized by three or four enveloping membranes is a widespread phenomenon. The secondary plastids of Euglenophyta and Chlorarachniophyta, which belong to the green algal lineage, have probably evolved polyphyletically by secondary endosymbioses between different host cells and green algal endosymbionts (Archibald and Keeling 2002; McFadden et al. 1994). In contrast, secondary plastids descending from a red algal endosymbiont occur in Cryptophyta, Haptophyta, Heterokonta (including the Heterokontophyta), and Alveolata (Cavalier-Smith 2002). As the plastids of the latter four taxa were suggested to share a common photobiotic ancestor, these taxa were collectively designated the chromalveolates (Cavalier-Smith 1999, 2003). The development of heterotrophic organisms within this group was explained by plastid loss or degradation (Andersson and Roger 2002; Saldarriaga et al. 2001).

The hypothesis of a monophyletic origin of the chromalveolates is supported by phylogenetic analyses of the plastid-targeted enzymes glyceraldehyde-3-phosphate dehydrogenase and fructose-1,6-bisphosphate aldolase (Harper and Keeling 2003; Patron et al. 2004). Likewise, corroborating molecular studies of multiple plastid genes (Bachvaroff et al. 2005; Yoon et al. 2002, 2004) and nuclear gene analyses (Harper et al. 2005; Li et al. 2006) point to a close phylogenetic relationship between certain chromalveolate taxa. Considering the high variety of chromalveolate living forms and their substantial morphological differences, however, the monophyletic origin of the chromalveolates remains debatable. Thus, it was intensely discussed whether the chromalveolates could have developed polyphyletically from several secondary endosymbiontic events rather than from one single endosymbiosis (Falkowski et al. 2004; Grzebyk et al. 2004; Keeling et al. 2004), but evidence reliably supporting this scenario is hitherto missing. The discovery of the Synchromophyceae with their unique multiplastidic secondary endosymbionts substantially contributes to the discussion about the evolution of the chromalveolates since the Synchromophyceae plastid complexes morphologically differ from the single secondary plastids of all other chromalveolate taxa.

Results

Analyses of the 18S rRNA and *rbc*L genes (GenBank accession numbers DQ788730 and DQ788731) identified *Synchroma grande* as a member of the Heterokontophyta. In all phylogenetic trees computed with maximum likelihood, Bayesian statistics, maximum parsimony and neighbour-joining, the sequences of *S. grande* were located within the Heterokontophyta, distinct from all other classes which were themselves often supported by high bootstrap and probability values (Figs 1 and 2). Moderate bootstrap and probability values indicated a phylogenetic sister group relationship between *S. grande* and the Chrysophyceae/Synurophyceae. However, the Chrysophyceae/Synurophyceae clade recovered with maximum or high support values in all trees never included *S. grande*.

Morphological studies showed that migrating, floating, and sessile stages of the life cycle of *S. grande* were amoeboid. Flagellate cells were missing. Viewed from above, migrating and floating amoebae had a spiny outline (Fig. 3A,D). A central spherical or fusiform cell portion of 10—25 μm length and sometimes only 7 μm width contained the nucleus and the plastids. It was surrounded by hyaline cortical plasma, the origin of axopodia-like pseudopodia which might be simple or laterally branched. Quickly migrating amoebae were fusiform and generally 55—130 (-200) μm long. At their anterior and posterior ends, they had groups of axopodia, sometimes up

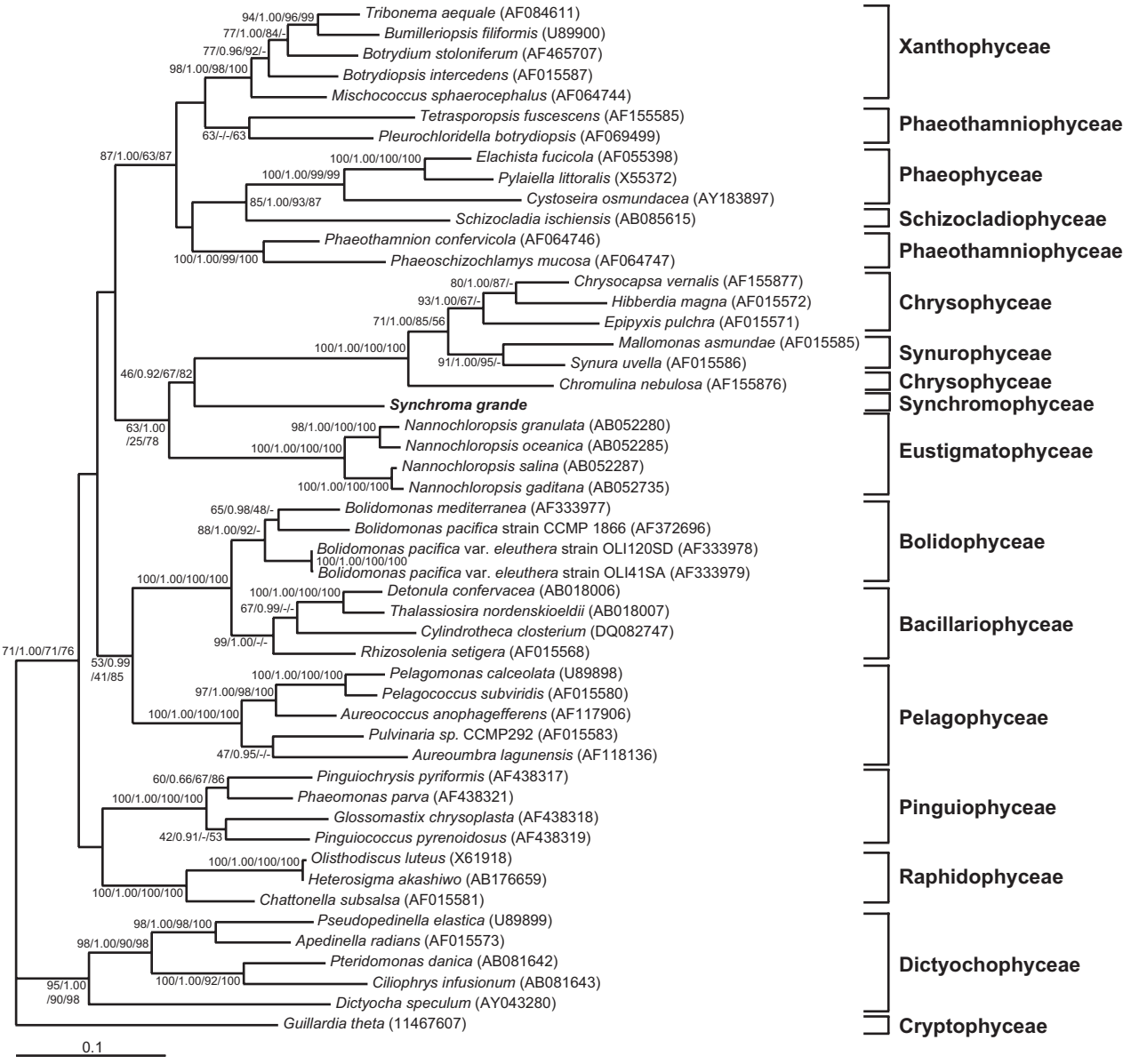

Figure 1. Phylogenetic tree of *rbc*L gene analyses for photobiotic Heterokontophyta. Maximum likelihood tree based on a 1110 bp alignment (including gaps), rooted with a Cryptophyceae sequence. Bootstrap and Bayesian probability values at branches for ML, Bayes, MP, and NJ are separated by slashes. Accession numbers of species included in the analyses are shown in round brackets.

to about 140 μm in length. Sessile cells cultured in a Petri dish (Fig. 3A,E,F) had an almost circular main cell body with a diameter of about 22 μm. Occasionally, main cell bodies with larger diameters occurred. The surrounding loricae (Fig. 3A,B,F) usually reached 26 μm in width but only 3—4 μm in height. Main cell bodies were locally attached to the loricae by protuberances of the cytoplasm. Loricae had one or less frequently 2—3 ostioles through which the reticulopodial part of the cell protruded. Plasmatic strands of the reticulopodia were 0.8—1.5 μm wide (Fig. 3A,E,F), but were much broader in plasmatic sheets. Reticulopodia of neighboring cells fused and formed a meroplasmodium (Grell et al. 1990) (Fig. 3A) that was able to catch and incorporate other organisms, e.g. bacteria and diatoms. Engulfed organisms or particles were observed to be digested in all parts of the plasmodial network (Fig. 3E). More often they were

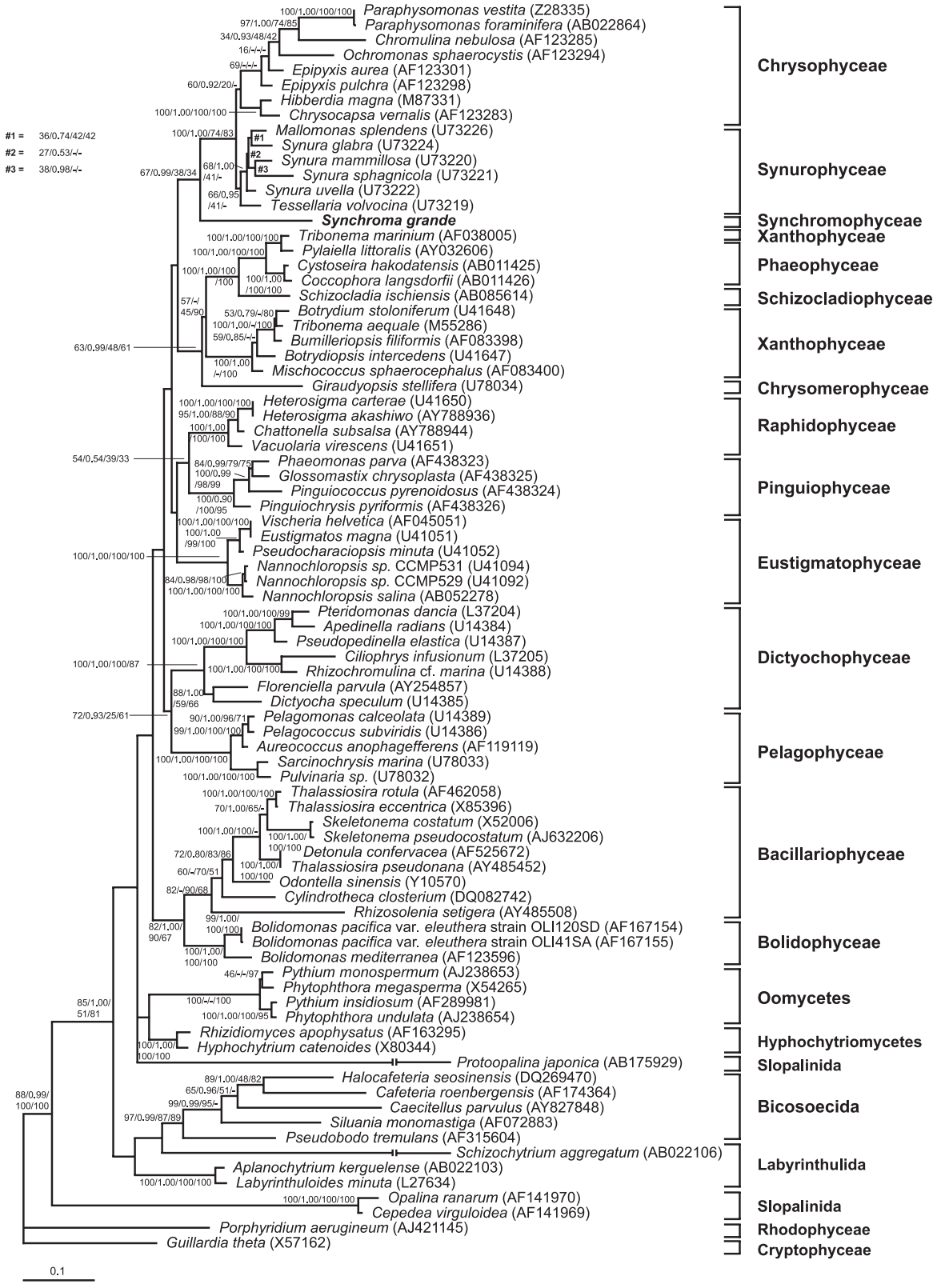

Figure 2. Phylogenetic tree of 18S rRNA gene analyses. Maximum likelihood tree based on a 1952 bp alignment (including gaps), rooted with a Cryptophyceae sequence. Bootstrap and Bayesian probability values at branches for ML, Bayes, MP, and NJ are separated by slashes. Accession numbers of species included in the analyses are shown in round brackets.

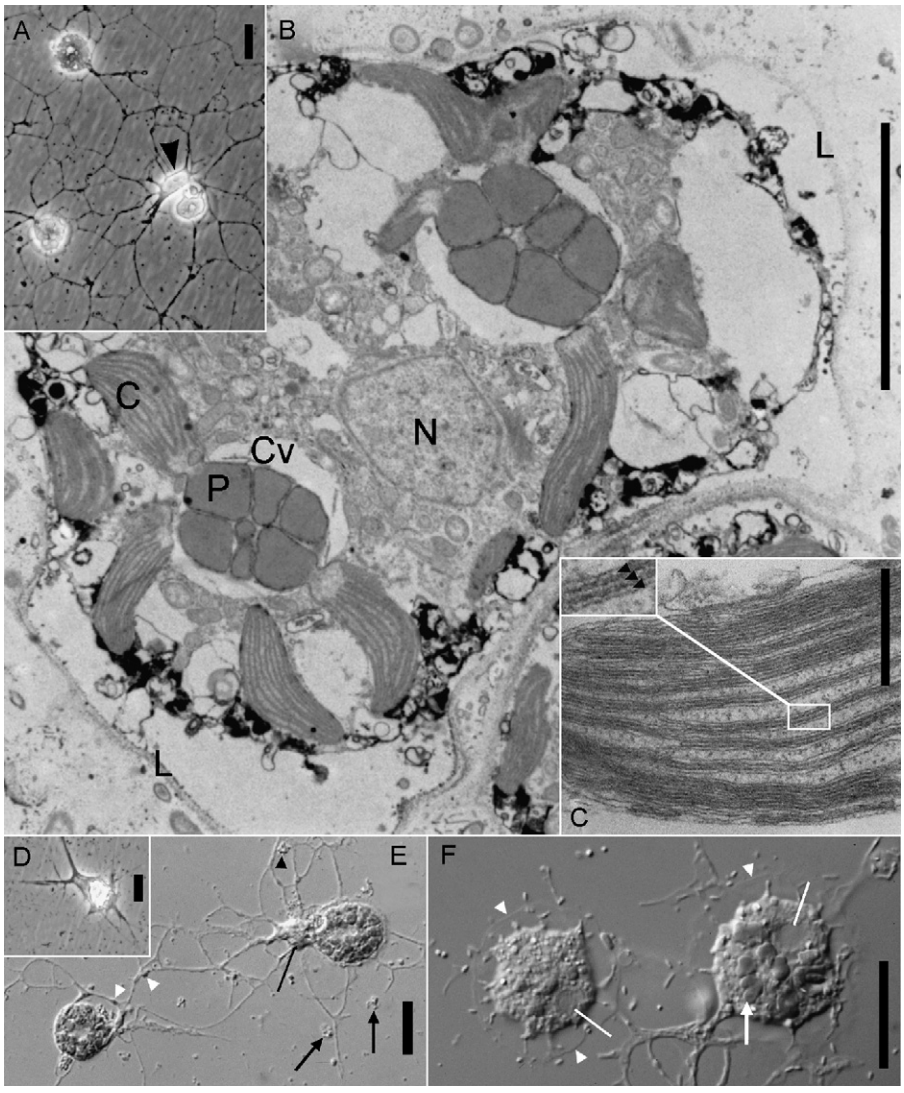

Figure 3. *Synchroma grande*. **A**. Phase-contrast light microscopical image; scale bar: 20 μm. The circular main cell bodies of the three sessile amoebae are surrounded by loricae appearing as faint shadows. The protruding reticulopodial strands of the cells are highly branched and are interconnected to form a meroplasmodium. After binary cell division of the sessile amoeba on the right, one daughter cell has hatched out of the lorica to become a migrating amoeba with a fusiform shape (arrowhead). **B**. Transmission-electron microscopical overview of a sessile amoeba; scale bar: 5 μm. Every chloroplast has a pigmented lobe (C) which is connected to the terminal pyrenoid (P). The pyrenoids of six neighboring chloroplasts are densely aggregated in the center of the radiating lobes and are surrounded by a capping vesicle (Cv). Two chloroplast aggregates representing multiplastidic secondary endosymbionts are visible in the cell. N: nucleus, L: lorica. **C**. Detail of a pigmented chloroplast lobe containing longitudinally arranged lamellae of three adpressed thylakoids which are marked by arrowheads in the enlarged insert; scale bar: 0.5 μm. **D**. Migrating amoeba with spiny outline; phase-contrast optics; scale bar: 20 μm. **E**. Two sessile amoebae interconnected by reticulopodia with engulfed organisms or particles (white arrowheads). Aggregates and remnants of the digesting vacuoles containing the engulfed materials occur within (black arrowhead) or outside (black arrows) of the meroplasmodial network. A particularly large accumulation of digesting vacuoles (black line) occurs outside of the lorica in front of the ostiolum; differential intereference contrast (DIC) optics; scale bar: 20 μm. **F**. Two sessile amoebae interconnected by reticulopodia. White arrowheads point to the loricae. Main cell bodies have a somewhat irregularly stellar outline due to protuberances of the cytoplasm attached to the lorica. Within the cells, nuclei are marked with white lines. A chloroplast complex in which the pyrenoids are densely aggregated in the center of the radiating lobes is clearly visible (white arrow); DIC optics; scale bar: 20 μm.

transported toward the main cell bodies. Digestion took place outside of the loricae in front of the ostioles where large aggregates of digesting vacuoles could be formed (Fig. 3E).

After binary cell division of the sessile amoebae, one daughter cell stayed within the lorica, whereas the second cell became a migrating amoeba (Figs 3A and 4). Migrating amoebae could also directly be formed from sessile amoebae which hatched out of their loricae. Sessile or floating amoebae developed from migrating amoebae.

In the cytoplasm of *S. grande*, mitochondria of the tubular type (Figs 5C,D and 6) were found near to endosymbiontic bacteria (Fig. 6). A unique feature in the photobiotic Synchromophyceae was the arrangement of the yellowish-green chloroplasts in groups. Every cell of *S. grande* possessed 2—4 planar or slightly cup-shaped aggregates with 6—8 chloroplasts each (Figs 3B,F and 5). Transiently, complexes with about 15 chloroplasts were observed. Cells with only one small or large chloroplast complex temporarily occurred, but were rarely observed. Every chloroplast had a terminal pyrenoid that was connected to the pigmented chloroplast lobe by a flattened stipe (Figs 3B and 5B). In a chloroplast complex, the pyrenoids were densely aggregated in the center of the radiating pigmented lobes (Fig. 3B), and were terminally covered by a single, dome-shaped capping vesicle (Figs 3B and 5C). Longitudinally arranged lamellae composed of three adpressed thylakoids were present in the pigmented lobes (Fig. 3C), which are a typical feature of many chlorophyll *c*-containing algae. HPLC pigment analyses of *S. grande* revealed the presence of chlorophylls *a* and c_2 (Table 1, Fig. 7) indicating a chromist ancestry. The simultaneous presence of fucoxanthin and the violaxanthin—antheraxanthin—zeaxanthin xanthophyll pigments (Table 1, Fig. 7) suggested a Heterokontophyta chloroplast type (Andersen 2004). A girdle lamella was evidently missing in the chloroplasts of *S. grande*. This feature clearly separates the new class Synchromophyceae from the Chrysophyceae and Synurophyceae which supports the results of the phylogenetic trees (Figs 1 and 2).

Every chloroplast of the Synchromophyceae was surrounded by two membranes and the whole chloroplast complex possessed two additional outer membranes (Fig. 5). The total of four enveloping membranes showed that the chloroplast complexes represent secondary endosymbionts. As the two outer membranes closely followed the outline of the chloroplast aggregate, the periplastidial compartment was narrow.

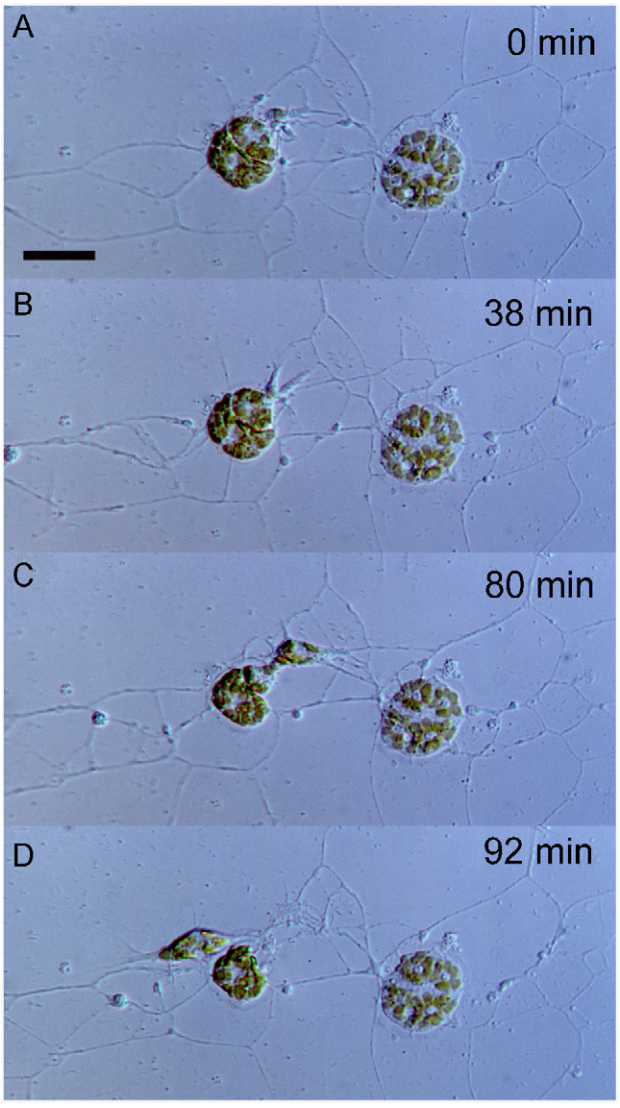

Figure 4. Light microscopical time-lapse documentation of the vegetative binary reproduction of a sessile amoeba (left cell) in a meroplasmodium of *Synchroma grande*. Scale bar: 20 μm. **A**. Binary division of the cell took place. **B**, **C**. One daughter cell hatches out of the lorica of the mother cell. **D**. The free daughter cell becomes a migrating amoeba while the second daughter cell remains sessile in the lorica of the mother cell. In the right cell, complexes of plastids with aggregated pyrenoids in their centers are visible. The plastid complexes are arranged around the middle of the cell; DIC optics. Cells were cultured in a plastic Petri dish with microscope cover glasses inserted in the bottom and the top.

Periplastid reticula could only be observed at particular sites, e.g. at the stipes (Fig. 5B) or between the tips of the pyrenoids (Fig. 5D).

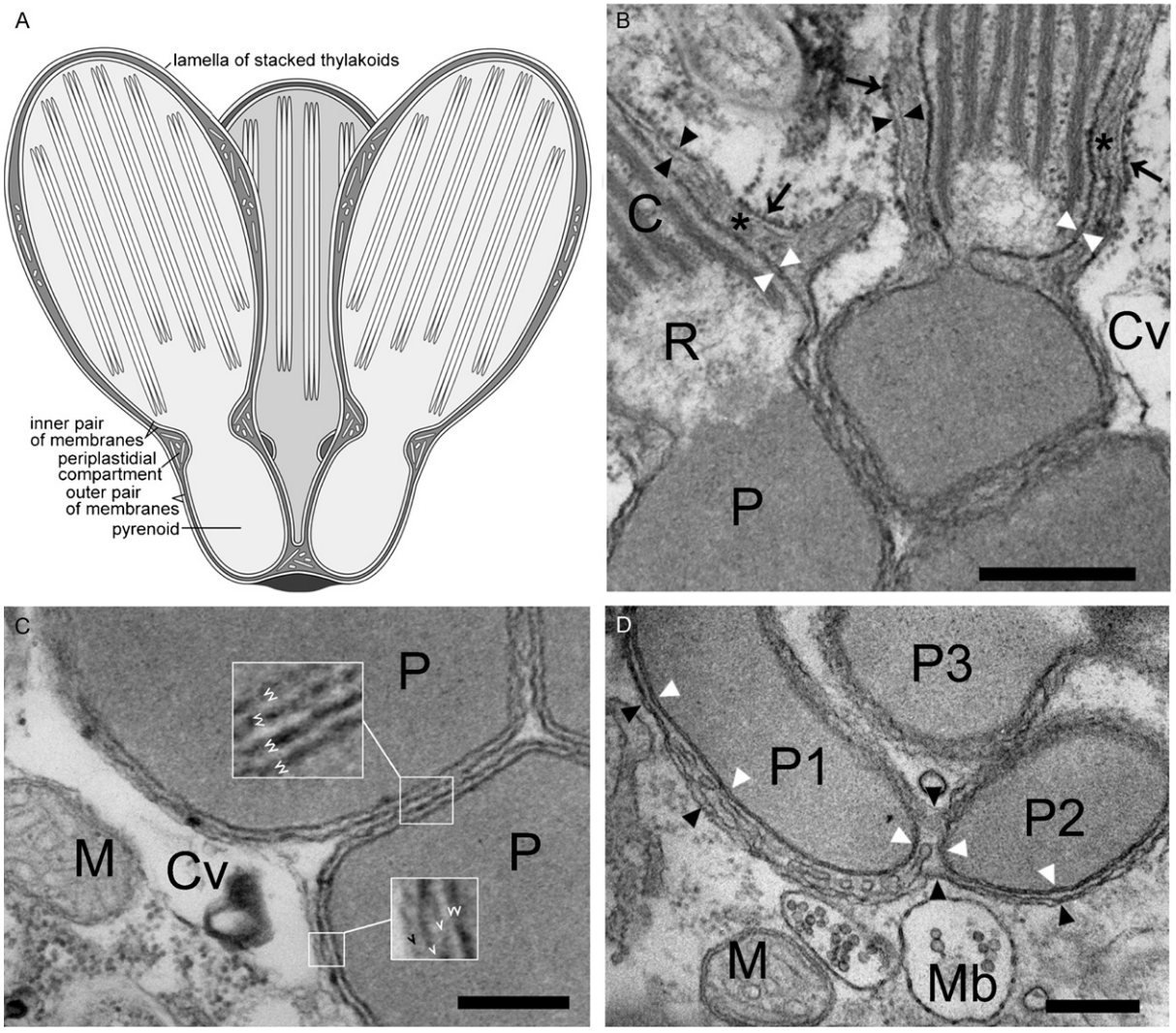

Figure 5. Substructure of the chloroplast aggregates in *Synchroma grande*. **A**. Schematic drawing summarizing the morphological observations. Several chloroplasts permanently share the outer pair of enveloping membranes that closely follows the outline of the chloroplast complex. The entire chloroplast aggregate constitutes a unity which represents a single, multiplastidic secondary endosymbiont. **B**. Pigmented chloroplast lobes (C), ending in electron-lucent regions in which lamellae are missing (R), are attached to the pyrenoids (P) by flattened stipes. Every chloroplast is enveloped by a pair of closely attached inner membranes (white arrowheads) and by an additional outer membrane pair (black arrowheads). The outermost membrane, called epiplastid rough endoplasmic reticulum, is studded with cytoplasmic ribosomes (arrows). The subjacent periplastid membrane borders the periplastidial compartment in which membrane-lined periplastid reticula occur (asterisks). In the region of the pyrenoids, the periplastidial compartment is particularly narrow. Scale bar: 0.5 μm; Cv: capping vesicle. **C**. Cross-sectional view of the chloroplast complex in the median plane of the pyrenoid region which is enclosed by a capping vesicle (Cv); scale bar: 0.3 μm. Every pyrenoid (P) is surrounded by four membranes which are arranged in closely attached pairs and are marked by inverted white arrowheads in the enlarged inserts. The additional membrane of the capping vesicle surrounding the pyrenoid complex is marked by a black inverted arrowhead. M: mitochondrion. **D**. Chloroplast complex longitudinally sectioned in the tip region of the pyrenoids; scale bar: 0.3 μm. The outer pair of enveloping membranes (black arrowheads) borders a corporate compartment enclosing two pyrenoids (P1 and P2) which themselves are surrounded by separate inner membrane pairs (white arrowheads). Membrane-lined periplastid reticula occur in the periplastidial compartment. The connection of pyrenoid P3 to the complex lies in a different plane and cannot be seen in this ultrathin section. M: mitochondrion, Mb: multivesicular body.

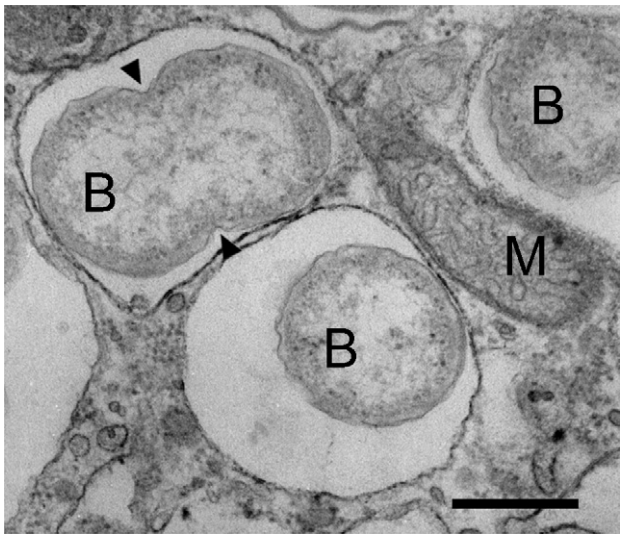

Figure 6. Cytological features of *Synchroma grande*. Bacteria (B) in membrane-lined compartments are proposed to be endosymbionts living within the host cell and reproducing by binary division (arrowheads). M: mitochondrion; scale bar: 0.4 μm.

Table 1. Isolated pigments of *Synchroma grande* in relation to the concentration of chlorophyll *a.*

Pigment	mM M^−1 Chlorophyll *a*
Chlorophyll c_2	136.61
Fucoxanthin	946.83
Violaxanthin	270.14
Antheraxanthin	43.69
Zeaxanthin	131.7
β-carotene	50.4

Taxonomic Treatments

Synchromophyceae Horn et Wilhelm class. nov. Algae eucaryoticae, chlorophyllis *a* et c_2. Cellulae compluribus chloroplastis flavo-virentibus in gregibus aggregatis; chloroplasti in parte pigmentifera lamellis longitudinalibus, sine lamella formae cinguli. Quisque chloroplastus duibus membranis internis vestitus, extra duibus membranis gregis chloroplastorum circumcinctus; inter membranas chloroplastorum et gregis reticulo periplastidico. Sequentiae geneticae rerum nominibus 18S rRNA gene et *rbc*L gene pro classe propiae.

Eukaryotic algae with chlorophylls *a* and c_2. Cells with several yellowish-green chloroplasts grouped in complexes; pigmented lobes of chloroplasts with longitudinally arranged lamellae, a girdle lamella is missing. Each chloroplast with two inner membranes, the whole plastid complex is surrounded by two outer membranes; a periplastidic reticulum exists between the membranes of the chloroplasts and the membranes of the complex. Nucleotide sequences of 18S rRNA and *rbc*L genes are distinctive.

Synchromales Schnetter et Ehlers ord. nov. Chloroplasti extremitate pyrenoide unica; pyrenoides chloroplastorum gregis omnino dense agglomeratae; pyrenoides agglomeratae vesicula galeanti unica gregis instructae. Cellulae sine flagellis.

Each chloroplast with one terminal pyrenoid; pyrenoids of chloroplast complexes are densely aggregated; the grouped pyrenoids are covered by a single capping vesicle. Cells without flagella.

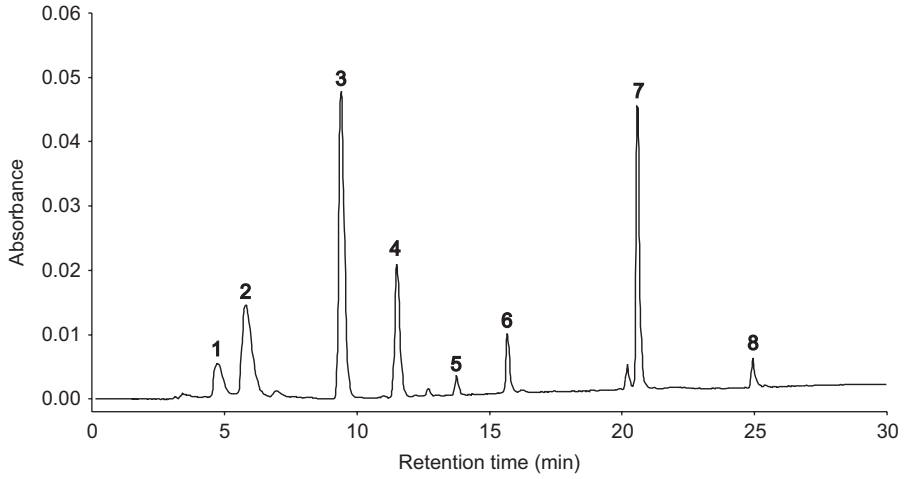

Figure 7. HPLC chromatogram of *Synchroma grande* at 440 nm. Retention time (min) on the *x*-axis and absorbance units on the *y*-axis. Peak identities: (1) chlorophyllide *a*, (2) chlorophyll c_2, (3) fucoxanthin, (4) violaxanthin, (5) antheraxanthin, (6) zeaxanthin, (7) chlorophyll *a*, and (8) β-carotene.

Synchromaceae Schnetter et Ehlers fam. nov. Corpus principale cellularum amoeboidearum sessilium loricam cingentem et reticulopodia faciens; cellulae amoeboideae migrantes et natantes axopodiis simplicibus vel ramosis. Mitochondria invaginationibus tubularibus.

Main cell body of sessile amoebae forms an enclosing lorica and reticulopodia; migrating and floating amoebae with simple or branched axopodia; mitochondria with tubular invaginations.

Synchroma Schnetter gen. nov. Algae eucaryoticae, chlorophyllis *a* et c_2. Corpora principalia cellularum amoeboidearum sessilium loricas cingentes et reticulopodiis conjunctis meroplasmodium facientia. Lorica in planitie applanata ostiolis lateralibus. Spatium inter loricam corporemque principale saepe protuberationibus cytoplasmatis. Chloroplasti in gregibus aggregati, per pyrenoides dense agglomeratas in area centrali gregum uniti, partibus pigmentiferis chloroplastorum radiantibus. Pyrenoides agglomeratae vesicula galeanti unica gregis instructae. Multiplicatio vegetativa cellularum meroplasmodii per bipartitionem effecta; filia una sedentaria in lorica manet, altera in amoebam migrantem vel natantem sine flagellis commutat.

Eukaryotic algae with chlorophylls *a* and c_2. Main cell bodies of sessile amoebae form enclosing loricae and a meroplasmodium by fusing reticulopodia. Lorica on plane surfaces flat with lateral pores. Space between lorica and main cell body frequently with protuberances of cytoplasm. Chloroplasts grouped in complexes, united by densely aggregated pyrenoids in the center of the complexes with radiating pigmented chloroplast lobes. Pyrenoid groups are covered by a single capping vesicle. Vegetative reproduction occurs by binary division; one daughter cell remains in the lorica of the mother cell, the second cell becomes a migrating or floating amoeba without flagella.

Synchroma grande Schnetter spec. nov. Corpora principalia cellularum meroplasmodii sessilia, in loricis incoloribus sine stratis ad substratum adnatis; in interstitiis formarum irregularium; in planitie lorica desuper applanata subcircularia, circiter 26 μm diametri et 3—4 μm alta, 1 rarius 2—3 ostiolis. Corpus principale circiter 22 μm diametri, aut interdum majus; in periphaeria protuberationibus cytoplasmatis aut chloroplastorum aliquantum irregulariter substellatum; reticulopodio e ostiolo loricae prodienti, cum reticulopodiis cellularum vecinarum conferruminato, filis circiter 0.8—1.5 μm latis, interdum latioribus et ad laminas facientibus, in margine plasmodii saepe recurvatis et inter se conjunctis. Corpora principalia plerumque 2—4 gregibus chloroplastorum planis vel calyculatis, 6—8 aut circiter 15 plastis compositis. Cellulae amoeboideae migrantes in amoeboideas sessiles aut natantes commutant.

Main cell bodies of the meroplasmodium are sessile, their not stratified colorless loricae are adpressed onto the substrate; form of the lorica is irregular in interstices; on plane surfaces, it has an almost circular outline when viewed from above; lorica about 26 μm in diameter and 3—4 μm high, with 1 or seldom 2—3 pores. Main cell body about 22 μm in diameter, occasionally larger; outline somewhat irregularly stellar, due to protuberances of the cytoplasm or caused by plastids; reticulopodia protrude from the pores of the lorica and fuse with those of neighboring cells, their strands are about 0.8—1.5 μm broad, occasionally broader and may form plasmatic sheets; plasmatic strands at the margin of the meroplasmodium recurved and fusing with each other. Main cell bodies generally with 2—4 plane or slightly cup-shaped plastid complexes composed of 6—8 or about 15 plastids. Migrating amoebae may transform into sessile or floating amoebae.

Holotype. Plastic embedded algal cells were deposited at the Herbarium of the Universidad de La Laguna, Tenerife, Spain (TFC), Phyc. no. 47701.

Type locality. The type material was collected in basaltic rocks from a large tide pool with sublittoral environmental conditions in the lower marine eulittoral near the lighthouse of Punta del Hidalgo, Tenerife, Canary Islands, Spain, by R. Schnetter in October 1993.

Etymology. The names of the class, order, and family were derived from the name of the genus which refers to the unique chloroplast complexes (syn-: Greek prefix, with, together; Chroma: Greek noun, color). The epithet *grande* pertains to the large cell size, compared to that of other species of the genus in our cultures which have not yet been described.

Discussion

The phylogenetic data (Figs 1 and 2) presented here suggest that the marine amoeboid alga *Synchroma grande* belongs to the Heterokontophyta and has a phylogenetic sister group relationship to the Chrysophyceae/Synurophyceae. To demonstrate that *S. grande* actually represents a new algal species that has not been described before, we directly compared *S. grande* with several genera which may be mistaken for

S. grande in light microscopical investigations (Table 2). The comparison is based on all genera treated by Kristiansen and Preisig (2001), who dealt with Chrysophyceae, Synurophyceae, Dictyochophyceae, Pelagophyceae, Phaeothamniophyceae, the colorless Bicosoecales (Bicosoecophyceae *nomen nudum*), and with genera of uncertain chrysophyte affinity.

To obtain a significant comparison of *S. grande* with those algal genera described in the late 19th century and at the beginning of the 20th century, we deliberately took into account characteristics and cellular structures that could only have easily been detected with the technical equipment of scientists working at that time, i.e. the habitat, the form of the lorica, and the number of chloroplasts per cell. Moreover, the comparison focuses on amoeboid genera of the above-mentioned algal taxa which form loricae, just as was observed in *S. grande*. Since Chrysamoebaceae (e.g. *Chrysidiastrum*, *Chrysamoeba*, *Chrysarachnion*, and *Chrysostephanosphaera*; cf. Kristiansen 2005; Kristiansen and Preisig 2001) do not form loricae, this family was excluded from the comparison. Moreover, cells of Chrysamoebaceae contain only (0-) 1—4 chloroplasts, i.e. fewer plastids than a cell of *S. grande*. Similarly, marine amoebae like *Rhizochromulina marina* were not included in Table 2 in cases when loricae were missing. This particular species also differs from *S. grande* in having only 1 chloroplast per cell and in forming flagellate life cycle stages (cf. Kristiansen and Preisig 2001).

Most genera, which are selected for Table 2 on the basis of the aforementioned criteria, are freshwater organisms with just (0-) 1—2 chloroplasts per cell, and therefore, clearly differ from *S. grande*. Loricate amoebae living in marine habitats like *S. grande*, have been described for the genera *Chrysopodocystis*, *Chrysothylakion*, and *Heliapsis*, only. *Chrysothylakion* and *Heliapsis* can unambiguously be distinguished from *S. grande* by the number of chloroplasts per cell (Table 2). *Chrysopodocystis socialis* (Billard 1978), the only species described so far in the genus *Chrysopodocystis*, resembles *S. grande* in having about 20 chloroplasts per cell. However, *S. grande* does not only differ from *Chrysopodocystis* in the shape of the lorica (Table 2), but in three more morphological features which are clearly discernable by light microscopy. First, in *Chrysopodocystis*, the chloroplasts are located in a parietal position (Billard 1978) and they are not organized in multiplastidic complexes with radiating pigmented lobes as was observed in *S. grande* (Fig. 3F). Second, the plastids of *S. grande* have large pyrenoids (Fig. 3F), whereas pyrenoids have not been detected in *Chrysopodocystis* chloroplasts (Billard 1978). Third, the lorica and the main cell body have no direct contact in sessile amoebae of *Chrysopodocystis* and they are separated from each other by an empty space (Billard 1978). In contrast, in sessile amoebae of *S. grande*, the main cell body is locally attached to the lorica by plasmatic strands called protuberances in the diagnosis (Fig. 3F). Thus, it is concluded that *S. grande*, in fact, represents a new species and that *Synchroma* is a new genus of loricate amoebae that does not correspond to any of the known genera. Further (ultra)structural, biochemical, and molecular studies on those amoeboid algal taxa already described in the past centuries would be valuable to validate their taxonomic classification (cf. e.g. Andersen 2004; Kawachi et al. 2002a) and to facilitate the adjustment of recent data.

A separate position of the genus *Synchroma*, clearly distinct from all classes of Heterokontophyta including the Chrysophyceae/Synurophyceae, is not only supported by the phylogenetic data (Figs 1 and 2), but also by morphological criteria. Stomatocysts, frequently observed in the Chrysophyceae and often used as a feature for taxonomic classification within this class, have never been observed with *Synchroma*. The lack of a girdle lamella in the chloroplasts of *Synchroma* is another feature which separates this genus from the Chrysophyceae/Synurophyceae. On the other hand, the absence of a girdle lamella is typical for all Eustigmatophyceae and for individual species of the Heterokontophyta classes Raphidophyceae and Pinguiophyceae (cf. Andersen 2004). Yet, the lack of chlorophyll *c* and fucoxanthin, the polygonal shape of the pyrenoids, and the presence of flagellate stages with large and specially constructed eyespots are attributes which are characteristic for Eustigmatophyceae (Hibberd and Leedale 1971; cf. Andersen 2004), but do not apply to *Synchroma. Synchroma* also differs from the Raphidophyceae in the lack of flagella and trichocysts (cf. van den Hoek et al. 1993). The Pinguiophyceae possess only 1 (-2) chloroplast(s) with membranes penetrating into the pyrenoids and can be distinguished from *Synchroma* by these properties (Kawachi et al. 2002b).

The reasons discussed so far, would already be sufficient to propose Synchroma to belong to the new algal class Synchromophyceae within the Heterokontophyta. Another feature supporting this separate systematic position is the pigment composition of Synchroma (Table 1, Fig. 7). Although the simultaneous presence of chlorophylls

Table 2. Comparison of *Synchroma grande* with chrysophyte genera presenting life cycle stages with loricate amoebae (data from Kristiansen and Preisig 2001).

Genus	Habitat freshwater (f) or marine (m)	Phases with 1 or more flagella	Lorica with apical (a) and/ or lateral (l) pore(s)	Form of lorica	Lorica with stalk	Number of chloroplasts per cell	Several chloroplasts united in complexes
Synchroma grande	**m**	–	l	**Flat**	–	**12 or more**	**+**
Bitrichia Woloszyńska	f	–	l	With 2—3 spines	–	1	–
Chrysoamphipyxis Nicholls	f	?	l	Ellipsoid with 2 lateral necks	–	1	–
Chrysoamphitrema Scherffel	f	?	l	Irregularly spherical	–	1—2	–
Chrysocrinus Pascher	f	–	a	Flat	–	1—2	–
***Chrysopodocystis* Billard**	**m**	–	l	**Spherical**	–	**about 20**	–
Chrysopyxis Stein	f	+	a	Roundish or bottle-shaped	–	1—2	–
Chrysothecopsis Conrad	f	–	l	Depressed spherical	–	1—2	–
***Chrysothylakion* Pascher**	**m**	**?**	**Lateral neck with pore**	**Ellipsoid flattened**	–	**2**	–
Derepyxis Stokes	f	+	a	Tubular, flask- or vase-shaped	+	1—2	–
***Heliapsis* Pascher**	**f, m**	–	l	**Lenticular**	–	**2, reduced, or 0**	–
Heliochrysis Pascher	f	?	a, l	Spherical	–	1—2	–

Table 2. (*continued*)

Genus	Habitat freshwater (f) or marine (m)	Phases with 1 or more flagella	Lorica with apical (a) and/or lateral (l) pore(s)	Form of lorica	Lorica with stalk	Number of chloroplasts per cell	Several chloroplasts united in complexes
Heterolagynion Pascher	f	–	a	Flattened	–	0	–
Hyalocylix Petersen et Hansen	f	?	a	Cylindrical or spherical, base narrow	+	1	–
Kybotion Pascher	f	+	l	flask-shaped	–	1–2	–
Lagynion Pascher	f	+	Apical neck with pore	flask-shaped	–	1–2	–
Palatinella Lauterborn	f	+	a	Inverse conical	+	1	–
Platytheca Stein	f	?	l	Flask-shaped	–	0	–
Porochrysis Pascher	f	?	Pores in posterior part	Ellipsoid	–	1, reduced	–
Porostylon Pascher	f	?	2 pores, l	Compressed spherical	+	1–2	–
Rhizaster Pascher	f	–	a	Cup-shaped	+	2	–
Stylochrysalis Stein	f	+	a	Ellipsoid	+	1–2	–
Stylococcus Chodat	f	–	a	Ellipsoid	+	1–2	–

a and *c* and characteristic xanthophylls suggests a close relationship of Synchroma to the Heterokontophyta, the presence of chlorophyll c_2 as the only chlorophyll *c* species is remarkable and has exclusively been found in dinoflagellates and cryptophytes so far (Larkum 2003). Yet, the chlorophyll *c* of the Heterokontophyta class Schizocladiophyceae has hitherto not been characterized, and chlorophyll *c* is entirely absent in the Eustigmatophyceae (cf. Andersen 2004).

The most striking and unique morphological feature of the Synchromophyceae, which was included in the formal description of the new class besides the phylogenetic and biochemical data, is the arrangement of chloroplasts into groups which share the outer pair of membranes. As such chloroplast complexes have never been described before for any other organism, the classification of the Synchromophyceae within the Heterokontophyta is conditionally. Further information about the new algal class Synchromophyceae is expected to come from detailed investigations of other algal isolates in our cultures, which presumably belong to the same taxon. So far, about 10 algal strains with evident morphological similarity to *S. grande* have been collected from marine habitats. Common features shared by all these strains were considered as characters of the higher-ranking taxa in our diagnoses. All types of secondary plastids known to date are surrounded individually by separate periplastidial compartments (Cavalier-Smith 2003). A unique and characteristic feature of the newly described Synchromophyceae is the occurrence of chloroplast complexes representing multiplastidic secondary endosymbionts. This conspicuous type of secondary endosymbiont is composed of several primary plastids that are permanently located in a common periplastidial compartment and are collectively enveloped by the periplastid membrane (PPM) and the epiplastid rough endoplasmic reticulum (EPrER) (Fig. 5).

The origin of the plastid complexes of the Synchromophyceae is an open question. Such plastid morphology could have evolved by abnormal division of conventional secondary Heterokontophyta plastids within the outer membrane pair, which appears to be a simple and obvious explanation. Yet, the question arises why the Synchromophyceae plastids should be retained together in a common compartment within the cytoplasm since this does not occur with all other multiplastidic Heterokontophyta.

Alternatively, the secondary endosymbiont of the Synchromophyceae could have derived from a multiplastidic red alga. This concept is problematic considering the monophyletic origin proposed for the secondary plastids in all chromalveolates, which is supported by molecular studies (Harper and Keeling 2003; Patron et al. 2004; Yoon et al. 2002). Assuming a common endosymbiontic ancestor derived from a multiplastidic red alga would imply that all chromalveolates, except for the Synchromophyceae, must have reduced their secondary plastid complexes to single secondary plastids. As this scenario appears unlikely, the discovery of multiplastidic red secondary endosymbionts can stimulate the discussion of whether a secondary endosymbiontic event involving a red alga actually took place only once in evolution; this issue is still a matter of debate (Falkowski et al. 2004; Grzebyk et al. 2004; Keeling et al. 2004).

Irrespective of how the chloroplast complexes have evolved, their astonishing morphology might be of vital importance for the physiological control of the plastids. The single secondary plastids of heterokont algae described to date, are reached by congeneric regulatory signals in a discrete manner. In contrast, in the Synchromophyceae, a higher level of synchronization may be exerted by signals targeting the plastids within a plastid complex. After passing the common EPrER and PPM, regulatory signals enter the periplastidial compartment shared by several plastids. Thus, the signals simultaneously reach the plastids within the complex at once, likely allowing a more isochronal, coordinated activity. The simultaneous control of the chloroplasts belonging to one complex might be advantageous, especially for a supposed synchronization of plastid division within the complexes (data not shown). As previously discussed for other types of secondary plastids, further investigations are required in order to understand the recruitment of plastid division machinery components and associated mechanisms (Hashimoto 2005). This applies in particular to the secondary plastid aggregates of the Synchromophyceae where the identification of the division constituents can also deliver insights into the evolution of these secondary endosymbionts. Further work on the Synchromophyceae should focus on the evolution and physiology of the secondary plastid complexes.

Methods

Field work, isolation of the species, and cell culture: At the type locality, samples of benthic

microorganisms were scraped off from basaltic rocks of a large tide pool near low-tide level. Samples were cultivated in seawater from the collection site in plastic Petri dishes. Several times per week, the initial cultures were checked with an inverted Fluovert FU microscope (Leica Vertrieb, Bensheim, Germany) equipped with Leica PL Fluotar 10/0.30, NPL Fluotar L 25/0.35, and NPL Fluotar L 40/0.60 PHACO objective lenses. Relevant amoeboid algae were removed from the initial cultures with a plastic pipette and transferred separately into fresh seawater. After repeated isolation steps, unialgal cultures were obtained, which were then cultured in von Stosch's enriched seawater medium adjusted to a salinity of 33‰ (Schnetter et al. 1984). Cell culture of the so far only isolate of *Synchroma grande* (code E) was performed in Petri dishes at 20 °C and a light intensity of 1.2—50 μmol photons m^{-2} s^{-1} in a 12:12 h (L:D) photoperiod (cf. Beutlich and Schnetter 1993). The strain has been deposited in the Provasoli-Guillard National Center for Cultures of Marine Phytoplankton (CCMP) and is available under the strain number CCMP2876. A voucher culture is maintained by R.S.

DNA extraction and PCR amplification: Genomic DNA was extracted using a Chelex method (Regensbogenova et al. 2004). PCR amplification was performed using the Promega PCR Core System II (Mannheim, Germany) with primers and cycling protocol listed in the Tables 3 and 4. Negative controls, without DNA, were run to ensure the absence of contamination and each PCR product was retrieved twice in independent reactions.

Cloning and sequencing: PCR products were cloned into a pCR 4-TOPO vector using a TA Cloning Kit for sequencing (Invitrogen, Karlsruhe, Germany) according to the manufacturer's instructions. Plasmid DNA was extracted from E. coli TOP10 chemically competent cells using the E.Z.N.A. Plasmid Miniprep Kit I (PeqLab, Erlangen, Germany). Sequencing of at least four clones from each PCR product was performed using a big dye terminator system (v 3.1 Applied Biosystems, Foster City, USA) and the primers M13F, M13R, T3, and T7 (Table 3). The obtained clone sequences from each gene showed polymorphic sites, for which the most frequent nucleotides were approved by direct sequencing of PCR products. The consensus sequences for the *rbc*L and 18S rRNA genes of *S. grande* are deposited in GenBank with the accession numbers DQ788730 and DQ788731.

Phylogenetic analyses: The analyses are based on a 1110 bp alignment of 50 *rbc*L genes and a 1952 bp alignment of 83 18S rRNA genes, including gaps. Sequences of *Guillardia theta* were used as outgroups. Alignments across taxa

Table 4. PCR cycling protocol.

Step	Conditions	Number of cycles
Denaturation	5 min at 95 °C	1
Denaturation	30 s at 95 °C	35
Annealing	"30 s at 45 — 55 °C	35
Elongation	1 to 2 min at 72 °C	35
Final elongation	7 min at 72 °C	1

Table 3. PCR primers.

Gene	Primer	
18S	srRNA6F	5′- GAT TAA GCC ATG CAY GTC TRA G -3′
	srRNA6F2	5′- GAG GTA GTG ACA ATA AAT AAC -3′
	srRNA6R	5′- GTG TGT ACA AAG GGC AGG GAC -3′
*rbc*L	rbcL_het_F1	5′- AAA AGT GAC CGT TAY GAA TC -3′ (modified from Daugbjerg and Andersen 1997)
	rbcL_het_R1 b	5′- GTT GWG AGT TAA TGT TTT CAT C -3′
	rbcL_het_F2 b	5′- GGA AAA AAY TAT GGT CGT GTA G -3′
	rbcL_het_R2 b	5′- GRA TAC CAC CAG ARG CWA CWG -3′
For colony PCR and sequencing		
M13fwd (-20)	5′- GTA AAA CGA CGG CCA G -3′	
M13rev	5′- CAG GAA ACA GCT ATG AC -3′	
T7	5′- TAA TAC GAC TCA CTA TAG GG -3′	
T3	5′- ATT AAC CCT CAC TAA AGG GA -3′	

were made using the ClustalW algorithm (Thompson et al. 1994) with default parameters implemented in the program package MEGA 3.1 (Kumar et al. 2004). To find the most appropriate model and parameters of DNA nucleotide substitution, we performed a hierarchical likelihood-ratio test with MODELTEST v.3.7 (Posada and Crandall 1998). The GTR model (Lanave et al. 1984; Rodriguez et al. 1990; Tavare 1986; Yang 1994) combined with a proportion of invariable sites $I = 0.3357$ and a gamma distribution shape parameter $G = 0.9482$ was the best fitting model of 56 tested models for the *rbc*L analyses and the Tamura—Nei model (Tamura and Nei 1993) with a proportion of invariable sites $I = 0.2916$ and a gamma distribution shape parameter $G = 0.5453$ was the best fitting model of 56 tested models for the 18S rRNA gene analyses. The selected model and parameters were used to perform neighbor-joining (NJ), maximum-likelihood (ML), and Bayesian analyses. Based on the selected model, we estimated the discrete-gamma model to accommodate rate variation among sites and the parameter of invariable sites separately with the algorithm implemented in the program PHYML (Guindon and Gascuel 2003). Phylogenetic relationships were estimated with NJ and maximum parsimony (MP) using PAUP*4.0b10 (Swofford 2003) and ML using PHYML and Bayesian analysis using MRBAYES v3.1.2 (Ronquist and Huelsenbeck 2003). For all reconstructions except Bayesian analysis, the robustness of the branching pattern was tested by bootstrapping (Felsenstein 1985). For MP analysis, 2000 bootstrap replicates and a permutation test with 100 steps were conducted. For ML analysis, 2000 bootstrap replicates were run. For ML and MP analyses, we used the heuristic search method with 10 random stepwise additions and the TBR branch-swapping option. Bayesian analyses were run for 1 000 000 generations, with a print frequency of 100 and a sampling frequency of 10 generations. From the 100 000 trees found, we determined a subset of trees for building our consensus tree by inspecting likelihood values of trees saved by MRBAYES and set the burn-in option to 10 000 trees discarded to ensure stable likelihood values were achieved.

Light microscopy: Light microscopy was performed as previously described (Dietz et al. 2003). For light microscopic photographs, an inverted Leica (Leica Vertrieb, Bensheim, Germany) Fluovert FU microscope was used. Phase contrast photographs (Fig. 3A,D) were taken with Leica NPL Fluotar L 25/0.35 and NPL Fluotar L 40/0.60 PHACO objectives, respectively. For Figures 3E and 4 (DIC), a Leica EF 50/0.85 P objective with additional DIC optics was used. The numerical aperture of the condenser was 0.50. Figure 3F (DIC) was taken with a Leica Dialux 20 microscope, equipped with a NPL Fluotar 100/1.32 ICT objective. Camera: Leica (Wild) Photoautomat MPS 45/51 S. Film: Agfa CTp 100.

Fixation procedures (cf. Dietz et al. 2003): For transmission electron microscopy, cells were cultured in 55 mm-polystyrene Petri dishes on a thin layer of 2% (w/v) agar in seawater and covered with seawater. Fixation was performed within the Petri dishes in seawater containing 0.5% (v/v) glutardialdehyde (pH 8) for 2 h at room temperature. After washing in seawater, smaller samples were cut out of the agar layer, and the cells on top of the agar pieces were immediately covered with 2% (w/v) low-gelling agarose (type VII, Sigma-Aldrich Chemie, München, Germany) in distilled water. Samples were post-fixed in 2% (w/v) OsO_4 in 0.1 M cacodylate buffer (pH 7.2) for 3 h at 4 °C. After being rinsed in distilled water and dehydrated in a graded ethanol series, samples were embedded in Spurr′s epoxy resin (Spurr 1969). Ultrathin sections were cut with a diamond knife on a Reichert Om U2 ultramicrotome (Leica Microsystems GmbH, Wetzlar, Germany), collected on Formvar-coated, single-slot copper grids, and stained with uranyl acetate and Reynolds′ lead citrate (Reynolds 1963).

Transmission electron microscopy: Ultrathin sections were examined with the Philips EM 300 electron microscope (Philips, Eindhoven, The Netherlands) of the Zentrale Biotechnische Betriebseinheit, Universität Gießen, at 80 kV. Photographs were taken with 35 mm b/w negative films (AGFAORTHO 25 or MACO ORTHO 25).

Photograph processing: Light and electron microscopic photographs presented in this publication were scanned with a resolution of 1800 dpi using an Epson Perfection 4180 Photo Scanner and Epson Scan v2.50G. Color depth was 8-bit grayscale. For Figure 4, resolution and color depth were 1200 dpi and 24-bit color, respectively. Digital images saved as tif files were further processed with Corel PHOTO PAINT v7. Processing included image enlargement and simultaneous reduction of the resolution to 800 dpi, careful error-correction with the help of a cloning tool (only in those parts of the TEM images which do not show essential information), changes in brightness and contrast in order to attain equal levels of the panels assembled in the same figure, and labeling of the images.

Primary magnifications of LM slides, TEM—negatives, and scan-originals were: Figs. 3A, 3D: 100 x, Figure 3B: 1320 x, Figure 3C: 11550 x, Figure 3E: 200 x, Figure 3F: 400 x, Figure 4: 200 x, Figure 5B: 9240 x, Figure 5C: 14850 x, Figure 5D: 11550 x, and for Figure 6: 11550 x .

Pigment analysis: Cells were filtered and HPLC analyses were carried out as previously described (Wilhelm et al. 1995). Identification of the peaks was performed by comparing retention times and on-line spectra of pigment fractions with those of authentic standards.

Acknowledgements

We thank Cornelia Dietz (Giessen) for her support during early stages of this work and Martin Schlegel (Leipzig) for helpful discussion. For EM, we used the equipment of the Zentrale Biotechnische Betriebseinheit, Universität Giessen.

References

Andersen RA (2004) Biology and systematics of heterokont and haptophyte algae. Am J Bot **91**: 1508—1522

Andersen RA, Potter D, Bailey JC (2002) *Pinguiococcus pyrenoidosus* gen. et sp. nov. (Pinguiophyceae), a new marine coccoid alga. Phycol Res **50**: 57—65

Andersson JO, Roger AJ (2002) A cyanobacterial gene in nonphotosynthetic protists – an early chloroplast acquisition in eukaryotes? Curr Biol **12**: 115—119

Archibald JM, Keeling PJ (2002) Recycled plastids: a 'green movement' in eukaryotic evolution. Trends Genet **18**: 577—584

Bachvaroff TR, Sanchez Puerta MV, Delwiche CF (2005) Chlorophyll c-containing plastid relationships based on analyses of a multigene data set with all four chromalveolate lineages. Mol Biol Evol **22**: 1772—1782

Beutlich A, Schnetter R (1993) The life cycle of *Cryptochlora perforans* (Chlorarachniophyta). Bot Acta **106**: 441—447

Billard C (1978) *Chrysopodocystis socialis* gen. et sp. nov. (Chrysophyceae), une nouvelle Rhizochrysidale marine loriquée. Bull Soc Bot Fr **125**: 307—312

Bongiorni L, Jain R, Raghukumar S, Aggarwal RK (2005) *Thraustochytrium gaertnerium sp*. nov.: a new thraustochytrid stramenopilan protist from mangroves of Goa, India. Protist **156**: 303—315

Cavalier-Smith T (1981) Eukaryote kingdoms: seven or nine? Biosystems **14**: 461—481

Cavalier-Smith T (1986) The Kingdom Chromista: Origin and Systematics. In Round FE, Chapman DJ (eds) Progress in Phycological Research. Biopress, Bristol, pp 309—347

Cavalier-Smith T (1999) Principles of protein and lipid targeting in secondary symbiogenesis: euglenoid, dinoflagellate, and sporozoan plastid origins and the eukaryote family tree. J Eukaryot Microbiol **46**: 347—366

Cavalier-Smith T (2002) The phagotrophic origin of eukaryotes and phylogenetic classification of Protozoa. Int J Syst Evol Microbiol **52**: 297—354

Cavalier-Smith T (2003) Genomic reduction and evolution of novel genetic membranes and protein-targeting machinery in eukaryote-eukaryote chimaeras (meta-algae). Phil Trans R Soc Lond Ser B **358**: 109—134

Daugbjerg N, Andersen R (1997) Phylogenetic analyses of the *rbcL* sequences from haptophytes and heterokont algae suggest their chloroplasts are unrelated. Mol Biol Evol **14**: 1242—1251

Dick MW (2001) Straminipilous Fungi. Kluwer Academic Publishers, Dordrecht

Dietz C, Ehlers K, Wilhelm C, Gil-Rodríguez MC, Schnetter R (2003) *Lotharella polymorpha* sp. nov. (Chlorarachniophyta) from the coast of Portugal. Phycologia **42**: 582—593

Eikrem W, Romari K, Latasa M, Le Gall F, Throndsen J, Vaulot D (2004) *Florenciella parvula* gen. et sp. nov. (Dictyochophyceae, Heterokontophyta), a small flagellate isolated from the English Channel. Phycologia **43**: 658—668

Falkowski PG, Katz ME, Knoll AH, Quigg A, Raven JA, Schofield O, Taylor FJR (2004) The evolution of modern eukaryotic phytoplankton. Science **305**: 354—360

Felsenstein J (1985) Confidence-limits on phylogenies – an approach using the bootstrap. Evolution **39**: 783—791

Grell KG, Heini A, Schüller S (1990) The ultrastructure of *Reticulosphaera socialis* Grell (Heterokontophyta). Europ J Protistol **26**: 37—54

Grzebyk D, Katz ME, Knoll AH, Quigg A, Raven JA, Schofield O, Taylor FJR, Falkowski PG (2004) Response to comment on "The evolution of modern eukaryotic phytoplankton". Science **306**: 2191

Guindon S, Gascuel O (2003) A simple, fast, and accurate algorithm to estimate large phylogenies by maximum likelihood. Syst Biol **52**: 696—704

Harper JT, Keeling PJ (2003) Nucleus-encoded, plastid-targeted glyceraldehyde-3-phosphate dehydrogenase (GAPDH) indicates a single origin for chromalveolate plastids. Mol Biol Evol **20**: 1730—1735

Harper JT, Waanders E, Keeling PJ (2005) On the monophyly of chromalveolates using a six-protein phylogeny of eukaryotes. Int J Syst Evol Microbiol **55**: 487—496

Hashimoto H (2005) The ultrastructural features and division of secondary plastids. J Plant Res **118**: 163—172

Hibberd DJ, Leedale GF (1971) A new algal class: the Eustigmatophyceae. Taxon **20**: 523—526

Kawachi M, Noel MH, Andersen RA (2002a) Re-examination of the marine 'chrysophyte' *Polypodochrysis teissieri* (Pinguiophyceae). Phycol Res **50**: 91—100

Kawachi M, Inouye I, Honda D, O'Kelly CJ, Bailey JC, Bidigare RR, Andersen RA (2002b) The Pinguiophyceae

classis nova, a new class of photosynthetic stramenopiles whose members produce large amounts of omega-3 fatty acids. Phycol Res **50**: 31—47

Kawai H, Maeba S, Sasaki H, Okuda K, Henry EC (2003) *Schizocladia ischiensis*: a new filamentous marine chromophyte belonging to a new class, Schizocladiophyceae. Protist **154**: 211—228

Keeling PJ, Archibald JM, Fast NM, Palmer JD (2004) Comment on "The evolution of modern eukaryotic phytoplankton". Science **306**: 2191

Kristiansen J (2005) Golden Algae. A Biology of Chrysophytes. ARG Gantner Verlag K.G., Ruggell

Kristiansen J, Preisig HR (2001) Encyclopedia of Chysophyte Genera. In Kies L, Schnetter R (eds) Bibliotheca Phycologica, vol. 110. J Cramer, Berlin Stuttgart

Kumar S, Tamura K, Nei M (2004) MEGA3: integrated software for molecular evolutionary genetics analysis and sequence alignment. Brief Bioinform **5**: 150—163

Lanave C, Preparata G, Saccone C, Serio G (1984) A new method for calculating evolutionary substitution rates. J Mol Evol **20**: 86—93

Larkum AWD (2003) Light-Harvesting Systems in Algae. In Larkum AWD, Douglas SE, Raven JA (eds) Photosynthesis in Algae. Kluwer Academic Publishers, Dordrecht, pp 277—304

Li S, Nosenko T, Hackett JD, Bhattacharya D (2006) Phylogenomic analysis identifies red algal genes of endosymbiotic origin in the chromalveolates. Mol Biol Evol **23**: 663—674

Massana R, Guillou L, Diez B, Pedros-Alio C (2002) Unveiling the organisms behind novel eukaryotic ribosomal DNA sequences from the ocean. Appl Environ Microbiol **68**: 4554—4558

McFadden G, Gilson P, Hofmann C, Adcock G, Maier U (1994) Evidence that an amoeba acquired a chloroplast by retaining part of an engulfed eukaryotic alga. Proc Natl Acad Sci USA **91**: 3690—3694

Moriya M, Nakayama T, Inouye I (2002) A new class of the stramenopiles, Placididea classis nova: description of *Placidia cafeteriopsis* gen. et sp. nov. Protist **153**: 143—156

O'Kelly CJ (2002) *Glossomastix chrysoplasta* n. gen., n. sp. (Pinguiophyceae), a new coccoidal, colony-forming golden alga from southern Australia. Phycol Res **50**: 67—74

Patron NJ, Rogers MB, Keeling PJ (2004) Gene replacement of fructose-1,6-bisphosphate aldolase supports the hypothesis of a single photosynthetic ancestor of chromalveolates. Eukaryot Cell **3**: 1169—1175

Patterson DJ (1989) Stramenopiles: Chromophytes from a Protistan Perspective. In Green JC, Leadbeater BS, Diver WL (eds) The Chromophyte Algae. Clarendon Press, Oxford, pp 357—379

Posada D, Crandall K (1998) MODELTEST: testing the model of DNA substitution. Bioinformatics **14**: 817—818

Regensbogenova M, Kisidayova S, Michalowski T, Javorsky P, Moon-Van Der Staay SY, Moon-Van Der Staay GWM, Hackstein JHP, McEwan NR, Jouany JP, Newbold JC, Pristas P (2004) Rapid identification of rumen protozoa by restriction analysis of amplified 18S rRNA gene. Acta Protozool **43**: 219—224

Reynolds ES (1963) The use of lead citrate at high pH as an electron-opaque stain in electron microscopy. J Cell Biol **17**: 208—212

Rodriguez F, Oliver JL, Marin A, Medina JR (1990) The general stochastic model of nucleotide substitution. J Theor Biol **142**: 485—501

Ronquist F, Huelsenbeck JP (2003) MrBayes 3: Bayesian phylogenetic inference under mixed models. Bioinformatics **19**: 1572—1574

Saldarriaga JF, Taylor FJR, Keeling PJ, Cavalier-Smith T (2001) Dinoflagellate nuclear SSU rRNA phylogeny suggests multiple plastid losses and replacements. J Mol Evol **53**: 204—213

Schnetter R, Ruckelshausen U, Seibold G (1984) Mikrospektralphotometrische Untersuchungen über den Entwicklungszyklus von *Ernodesmis verticillata* (Kützing) Børgesen (Siphonocladales, Chlorophyceae). Cryptogam Algol **5**: 73—78

Spurr AR (1969) A low-viscosity epoxy resin embedding medium for electron microscopy. J Ultrastruct Res **26**: 31—43

Swofford DL (2003) PAUP*: Phylogenetic Analysis Using Parsimony (* and other methods), version 4.0b 10. Sinauer Associates, Sunderland, Massachusetts

Tamura K, Nei M (1993) Estimation of the number of nucleotide substitutions in the control region of mitochondrial DNA in humans and chimpanzees. Mol Biol Evol **10**: 512—526

Tavare S (1986) Some probabilistic and statistical problems in the analysis of DNA sequences. Lect Math Life Sci **17**: 57—86

Thompson JD, Higgins DG, Gibson TJ (1994) CLUSTAL W: improving the sensitivity of progressive multiple sequence alignment through sequence weighting, position-specific gap penalties and weight matrix choice. Nucleic Acids Res **22**: 4673—4680

Yang Z (1994) Maximum likelihood phylogenetic estimation from DNA sequences with variable rates over sites: approximate methods. J Mol Evol **39**: 306—314

Yoon HS, Hackett JD, Pinto G, Bhattacharya D (2002) The single, ancient origin of chromist plastids. Proc Natl Acad Sci USA **99**: 15507—15512

Yoon HS, Hackett JD, Ciniglia C, Pinto G, Bhattacharya D (2004) A molecular timeline for the origin of photosynthetic eukaryotes. Mol Biol Evol **21**: 809—818

van den Hoek C (1978) Algen: Einführung in die Phykologie. Georg Thieme Verlag, Stuttgart

van den Hoek C, Jahns HM, Mann DG (1993) Algen. Georg Thieme Verlag, Stuttgart, New York

Wilhelm C, Volkmar P, Lohmann C, Becker A, Meyer M (1995) The HPLC-aided pigment analysis of phytoplankton cells as a powerful tool in water quality control. Water Res **44**: 132—141